Title

Single cell wound generates electric current circuit and cell membrane potential variations that requires calcium influx

Journal

Integrative Biology (United Kingdom), 6(7)

ISSN

1757-9694

Authors

Luxardi, G
Reid, B
Maillard, P
et al.

Publication Date

2014

DOI

10.1039/c4ib00041b

Volume 6 | Number 7 | July 2014 | Pages 647–728

Integrative Biology

Interdisciplinary approaches for molecular and cellular life sciences

www.rsc.org/ibiology

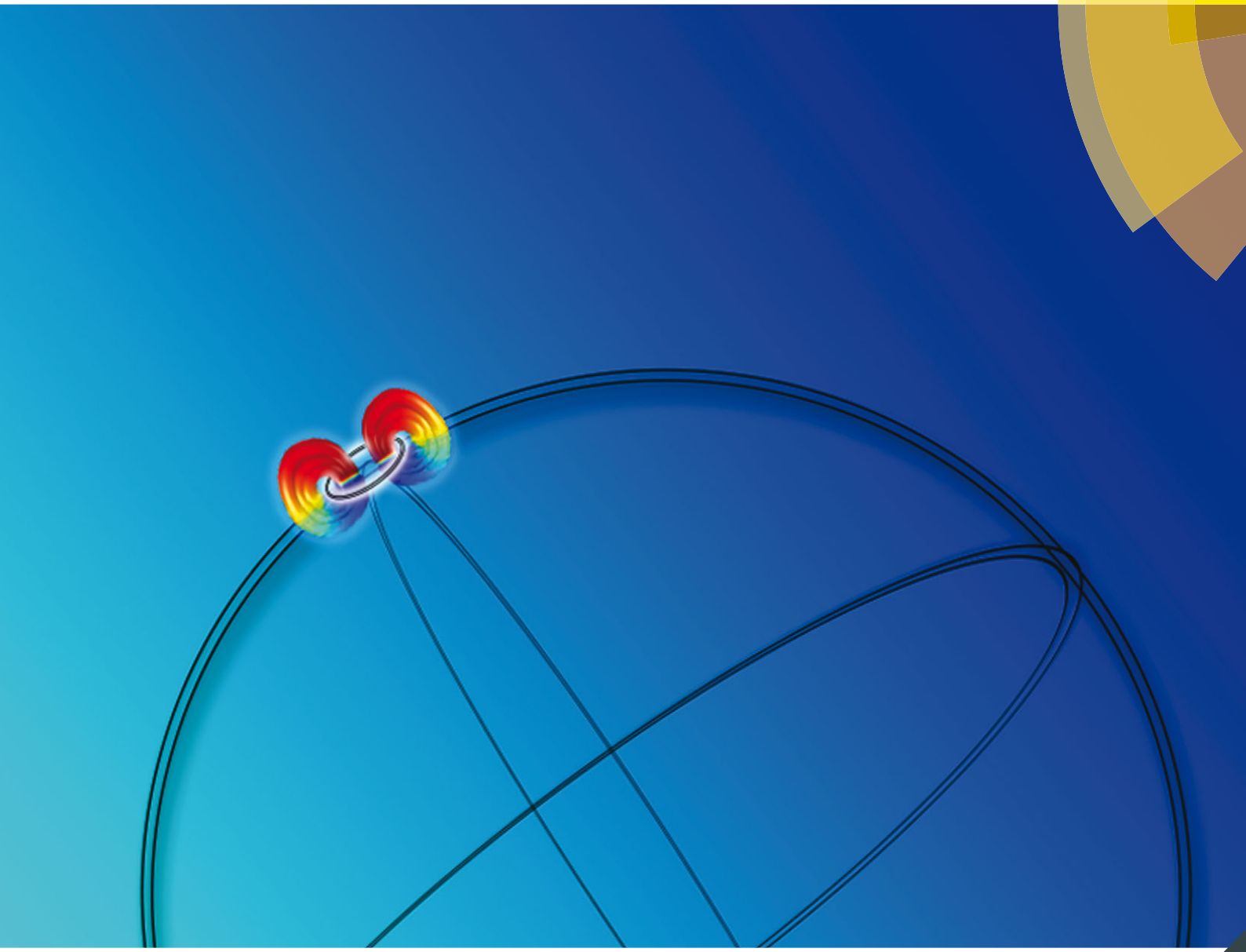

ISSN 1757-9694

ROYAL SOCIETY OF CHEMISTRY

PAPER

Guillaume Luxardi, Min Zhao *et al.*

Single cell wound generates electric current circuit and cell membrane potential variations that requires calcium influx

Integrative Biology

PAPER

View Article Online
View Journal | View Issue

Cite this: *Integr. Biol.*, 2014, 6, 662

Single cell wound generates electric current circuit and cell membrane potential variations that requires calcium influx†

Guillaume Luxardi,*[ab] Brian Reid,[ab] Pauline Maillard[c] and Min Zhao*[abd]

Received 21st February 2014,
Accepted 27th April 2014

DOI: 10.1039/c4ib00041b

www.rsc.org/ibiology

Breaching of the cell membrane is one of the earliest and most common causes of cell injury, tissue damage, and disease. If the compromise in cell membrane is not repaired quickly, irreversible cell damage, cell death and defective organ functions will result. It is therefore fundamentally important to efficiently repair damage to the cell membrane. While the molecular aspects of single cell wound healing are starting to be deciphered, its bio-physical counterpart has been poorly investigated. Using *Xenopus laevis* oocytes as a model for single cell wound healing, we describe the temporal and spatial dynamics of the wound electric current circuitry and the temporal dynamics of cell membrane potential variation. In addition, we show the role of calcium influx in controlling electric current circuitry and cell membrane potential variations. (i) Upon wounding a single cell: an inward electric current appears at the wound center while an outward electric current is observed at its sides, illustrating the wound electric current circuitry; the cell membrane is depolarized; calcium flows into the cell. (ii) During cell membrane re-sealing: the wound center current density is maintained for a few minutes before decreasing; the cell membrane gradually re-polarizes; calcium flow into the cell drops. (iii) In conclusion, calcium influx is required for the formation and maintenance of the wound electric current circuitry, for cell membrane re-polarization and for wound healing.

Insight, innovation, integration

Single cell wound healing is fundamental to maintain organ physiology after injury or in pathological disease conditions. The molecular aspects of single cell wound healing are partially understood, but its bio-physical counterpart has not been studied in detail. We hypothesize a bioelectric regulatory mechanism. Using *Xenopus laevis* oocytes as a model for single cell wound healing in combination with electrophysiological recording, we show that influx of calcium is required for wound electric current circuitry and cell membrane potential dynamics. The identification of electrophysiological regulation and control during single cell wound healing will have impact on our current understanding of how cells repair, provide a new experimental platform for studying bioelectricity of single cell wounds, and open new perspectives to restore or improve healing.

Introduction

Repair of cell membrane breach is a multi-step process and *Xenopus laevis* oocytes offer a powerful experimental model for study of single cell wound healing.[1] When *Xenopus laevis* oocytes are punctured, sealing of the wound requires disassembly of the cytoskeleton network beneath the wound. Removal of the cytoskeleton provides access to the wound by intracellular vesicles in order to bring new membrane and exocytosis quickly repairs the cell membrane. The cytoskeletal network is then remodeled and the membrane breach is fully repaired. The repair process requires calcium, its modulators such as calpain proteins, and also important modulators of the cytoskeleton such as the small GTPase, Cdc-42 and RhoA proteins.[2] Recent research has provided significant insights into the directional movement of vesicles, growth of cytoskeleton, and directional signaling of small GTPases.[3] An actomyosin contractile ring (controlled by concentric zones of the small GTPases Rho and Cdc42) is formed and closes to heal the cortical cytoskeleton.[3,4] The mechanisms by which vesicles move to the wound site, and how actomyosin ring contraction is initiated and controlled, are not well understood. Bement *et al.* demonstrated

[a] *Department of Dermatology, University of California Davis, 921 Stockton Blvd, Sacramento, CA 95817, USA. E-mail: minzhao@ucdavis.edu; Tel: +1 916 703-9381*
[b] *Institute for Regenerative Cures, University of California, 921 Stockton Blvd, Sacramento, CA 95817, USA. E-mail: gluxardi@ucdavis.edu; Tel: +1 916 703-9381*
[c] *Department of Neurology and Center for Neuroscience, University of California, Davis, Imaging of Dementia and Aging Laboratory, 1544 Newton Court, Davis, CA 95616, USA*
[d] *Department of Ophthalmology, School of Medicine, University of California Davis, 921 Stockton Blvd, Sacramento, CA 95817, USA*

† Electronic supplementary information (ESI) available. See DOI: 10.1039/c4ib00041b

that the centripetal signaling towards the center of the membrane breach does not depend on a myosin contraction ring.[3,4d] Contraction suppression does not prevent directional signaling such as activation of RhoA/cdc42 towards the center of cellular wounds in oocytes.[3] This closure is driven by a ''signal treadmill'' in which the GTPases are preferentially activated at the leading edges and preferentially lost from the trailing edges. How do these GTPase zones know front from back and segregate in different positions relative to the wound? A dual GEF-GAP-Abr regulates some of the features of Rho GTPase zones.[4d] For example, the abundance of F-actin ends or branch points may dictate GEF or GAP binding or activation.[3] One critical feature is the directional movement of vesicles, signal propagation, and actomyosin contraction. The mechanisms by which vesicles, signaling, actomyosin contractile array are directed precisely towards the wound center are not completely understood.

Surprisingly, very little is known about the potential role of electric currents and cell membrane potential during single cell wound healing. When giant axons from squid were severed, or ''bored'' in the context of sectioned spinal cord, large inward currents were measured at the stump end.[5] The inward electric currents decreased during the healing and returned to unwounded level when the membrane was resealed. This inward current is associated with an increase in intracellular calcium known to modulate cytoskeleton network dynamics through the regulation of its modulators.[4a,c] In addition, the membrane permeability to Cl^- is significantly increased.[6] Importantly, charges carried by molecules and membranes are known to act as localization cues inside the cell. It has been shown that cell membrane receptor concanavalin-a,[7] acetylcholine[8] and Epidermal Growth Factor (EGF) receptor can be redistributed along cell membranes by an applied electric field, demonstrating electrophoresis along cell membranes. In addition, it has been shown that exogenous molecules[9] as well as proteins[10] such as morphogens[11] can migrate through cell cytoplasm and gap junctions in an applied electric field. Finally, recent work led by Yeung *et al.* in 2008 showed that phospholipid dependent membrane charges borne by vesicles and plasma membranes can localize molecules such as the small GTPase based on the polybasic clusters and cationic domains of these proteins.[12] Interestingly, breaking the cell membrane is thought to lead to a massive entry of positively charged molecules and ions into the cell that could lead to the appearance of an inward electric current and cell membrane depolarization.[13]

We hypothesize that single cell wounding: (i) induces an electric current; (ii) causes cell membrane depolarization; (iii) induces a calcium influx that is required for electric current and membrane potential variations. In order to test these hypotheses, we used the *Xenopus laevis* oocyte[3,4,14] and electrophysiological recording.[15]

Materials and methods

Oocyte collection and handling

Ovary lobes or pre-sorted oocytes were purchased from Xenopus 1 (http://xenopus1.com). Lobes were separates manually using forceps in Barth's solution without calcium (88 mM NaCl, 1 mM KCl, 0.33 mM $Ca(NO_3)_2$, 0.41 mM $CaCl_2$, 0.82 mM $MgSO_4$, 2.4 mM $NaHCO_3$, 7.5 mM Tris-HCl, pH 7.4 and 0.1 mg ml^{-1} gentamicin) (Sigma-Aldrich, St. Louis, MO). Lobes were then transferred into a collagenase solution (0.012 g ml^{-1} of Barth's) for one hour and thirty minutes under slow agitation. When oocyte separation was achieved, or upon arrival of pre-sorted oocytes, stage VI oocytes were transferred into Barth's with calcium for overnight storage in an incubator at 13 °C prior to starting any experiments. Oocytes were then brought out of the incubating chamber to equilibrate to room temperature at least 30 min before starting any experiments.

Wound healing assay

The wounds were made by touching the oocyte membrane with a heat-pulled capillary microelectrode with a controlled tip diameter (53.3 ± 2.9 μm) mounted on a micromanipulator. The wound healing assays were performed in Mark's Modified Ringer (MMR 1×: 100 mM NaCl; 2 mM KCl; 2 mM $CaCl_2$; 1 mM $MgCl_2$; 5 mM Hepes; pH 7.5). Wound healing was monitored using time-lapse photography with a Ziess Lumar V12 microscope and wound area measured using Axiovision.

Vibrating probe measurements

Vibrating probes were prepared and used as previously detailed.[16] Briefly, the probe is an insulated stainless-steel needle with a platinum ball approximately 30 μm in diameter electroplated to the tip. The probe, mounted on a 3-dimensional micromanipulator, vibrated in solution about 10 μm from the oocyte cell membrane surface (Fig. 1A, ESI,† Fig. S2A–D and S5A) by a piezoelectric bender at a set frequency. If an electric (ionic) current was present, the charge on the platinum ball oscillates in proportion to the size of the current and at the frequency of vibration. The probe was attached to a lock-in amplifier that locked onto the probe's frequency signal, filtering out all other ''noise'' frequencies.

Prior to use, the probes were calibrated in the solution used for measurements (see below) with an applied current density of 1.5 μA cm^{-2}. It took approximately 30 seconds after wounding to position the vibrating probe. Measurements start one minute after wounding. Measurements were obtained at room temperature. Data were processed using WinWCP software.

Ion selective microelectrode measurement

Ion selective microelectrodes were prepared and used as previously detailed.[17] Borosilicate glass capillaries without filament were purchased from World Precision Instruments (WPI, Inc., Sarasota, FL, USA; cat #TW150-4). Silanization solution I (cat # 85126), calcium ionophore I cocktail A (cat # 21048), were obtained from Sigma-Aldrich (St. Louis, MO, USA). Borosilicate glass capillaries were heat-pulled using a one-step pull on a Narishige PC-10 electrode puller (Narishige International USA, Inc., New York, USA). Electrodes were heated in an oven (Model 10; Quincy Lab Inc., Chicago, IL, USA) and silanized to render the inside hydrophobic. Electrodes were stored in an electrode storage jar (WPI; cat # E215) inside a glass desiccator (Fisher Scientific, Pittsburgh, PA, USA; cat # 08-595D) containing desiccant

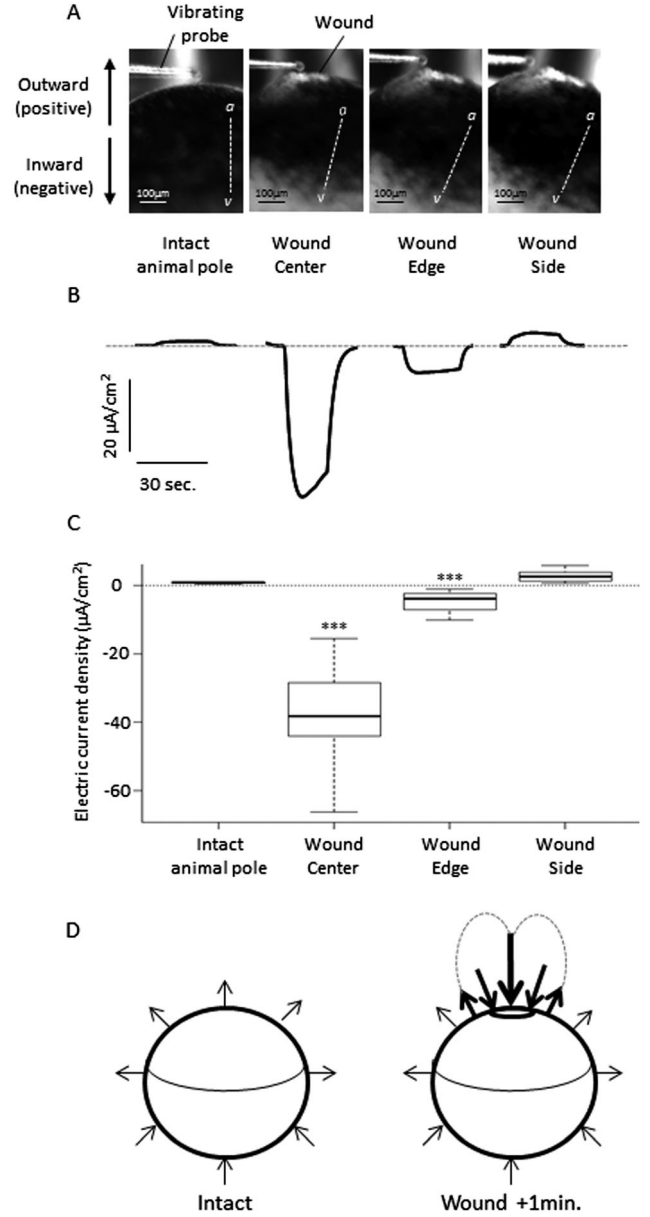

Fig. 1 Cell membrane wounds generate an electric current circuit. (A) Photograph illustrating electric current density measurements at intact cell membranes and wound center, edge and side using the vibrating probe. The dashed line between "a" and "v" represents the animal–vegetal axis (applies to subsequent figures). Arrows indicate the direction of the electric current represented by positive value when outward and negative value when inward in (B) and (C). (B) Example of electric current measurement traces obtained at the intact membrane, and one minute after wounding at the wound center, edge and side. The grey dashed line represents the zero level when the probe is in reference or 'bath' position. (C) Box plots showing electric current density distributions at intact membrane (n = 15), one minute after wounding at wound center (n = 20), edge (n = 10) and side (n = 18). (D) Scheme representing electric current at intact *Xenopus laevis* oocyte cell membrane and one minute after wounding. Arrows are not scaled to the measured density but do show the direction and relative sizes of the current density around the oocyte before and after wounding.

(Drierite; W.A. Hammond Drierite Co. Ltd, Xenia, OH, USA). Electrodes were back-filled with a solution containing 100 mM of $CaCl_2$. The electrode was then tip filled with a small amount (50–100 μm length) of the ionophore. Reference electrodes were glass capillaries as above and were filled with 3 M NaCl with 2% agar. Reference electrodes were mounted in a straight microelectrode holder with a gold 2 mm male connector and Ag/AgCl pellet (WPI; cat # MEH3S) and mounted on a 3-dimensional micropositioner (Newport Corporation, Irvine, CA, USA). Measuring electrodes were mounted in a straight microelectrode holder with a gold 1 mm male connector and Ag/AgCl wire (Warner Instruments, Holliston, MA, USA; cat # QSW-A15P) and attached to a head stage mounted on a computer-controlled electronic 3-dimensional micropositioner (Newport). The measuring electrode and reference electrode were connected to an Ion Amp V3.0 amplifier (BioCurrents Research Center, Woods Hole, MA, USA).

Electrodes were calibrated in standard solutions that bracketed the concentration of calcium present in solutions used for measurements (see below). The calcium electrode was calibrated in 0.1, 1, 10, 100 mM and 1 M $CaCl_2$. Plotting the logarithm of the molar concentration against the output of the amplifier (in mV) gave a linear fit with an R^2 value of 0.99 or greater. The formula describing the line was used to convert the mV readings from the amplifier during sample measurements into actual ion concentrations from which ion flux was finally calculated.

First, the oocytes were placed in a petri-dish containing the solution of interest at room temperature under the dissecting microscope for one minute before flux measurement. During this minute, the reference and measuring electrodes were placed in the bath. With the electrode at reference (bath) position (approximately 1 cm from the oocyte), the background value was recorded for one minute. The electrode was then moved into measuring position about 10 μm from the intact, unwounded cell membrane for 10–15 seconds until the new value was stable. Electrodes were used in self-referencing mode, where the electrode moves between two points 100 μm apart at low frequency (0.3 Hz) near the wound center, edges, sides or intact cell membrane (Fig. 4A, ESI,† Fig. S3A and S4A). The electrode movement was controlled by IonView32 software (BioCurrents Research Center). The electrode paused at each position ('Close' and 'Distant' noted C and D in Fig. 4B, ESI,† Fig. S3B) and the output was recorded. When a calcium flux was present, the electrode detected a difference in ion concentration between the two positions (Fig. 4B, ESI,† Fig. S4B). The ion flux was calculated using Fick's law of diffusion formula: $J = Cu\left(\frac{dc}{dx}\right)$ where C is the ion concentration in the solution, u the ion mobility, and dc the concentration difference over distance dx. Ion flux data are presented in nM cm^{-2} s^{-1}. Data were recorded using IonView32 software. Measurements at intact membrane were obtained for at least 3 minutes, allowing the oscillation to stabilize. For time-lapse experiments during wound healing, oscillations were recorded at the position of interest for the whole time course and data extracted using IonView32.

Glass microelectrode measurement

Borosilicate glass capillaries without filament were purchased from WPI as above. Borosilicate glass capillaries were two-step

heat-pulled using a Narishige PC-10 electrode puller. Electrodes were back-filled with 3 M KCl. The microelectrode was then placed onto a holder (Warner Instruments, Holliston, MA, USA) containing an Ag/AgCl wire immerged in the KCl solution. The holder with the microelectrode was inserted in the head stage of the voltage-clamp amplifier (Warner Oocyte Clamp OC-725C).

Using the micro-positioners, the tip of the microelectrode mounted on the holder was immersed into the solution of interest, *e.g.* MMR 1×, within the oocyte chamber. Microelectrodes had a resistance <1 MΩ. The microelectrode was then moved close to the intact membrane, adjusting the voltage reading on the amplifier to 0 mV. The oocytes were impaled with the microelectrode and resting membrane potential (in mV) recorded. PCLAMP software suite, including CLAMPEX and CLAMPFIT, were used for data acquisition and extraction, using a sampling rate of 100 Hz.

Modulation of extracellular calcium concentration

Control solution was MMR 1× (see above). Ion selective probe measurement of calcium concentration in the MMR 1× solutions used for the present work indicated mean ± SE values of 0.66 ± 0.03 mM (n = 4). Low calcium solution consisted of MMR 1× without added $CaCl_2$. $CaCl_2$ were not replaced by similar amount of choline-chloride as the absence of $CaCl_2$ did not dramatically change the chloride concentration (about 0.97 times). Ion selective probe measurement of calcium concentration in the different low calcium solutions were 0.04 ± 0.006 mM (n = 3). EGTA solutions contained MMR 1× supplemented with 5 mM EGTA (Sigma-Aldrich, St. Louis, MO). Surprisingly, the ion selective probe measurement of calcium concentration in the EGTA solutions used in the present work were similar to that of control solution (0.62 ± 0.07 mM, n = 3). Oocytes were placed in those solutions one minute before starting any experiments unless specified (wounding and electrophysiological measurements).

Statistical analyses

We used an ANOVA with mixed effects to assess for control condition models the independent effects of (1) the position of the vibrating probe on electric currents density and (2) the time on electric current, membrane potential and calcium influx; and for models with different calcium concentrations (normal, low or EGTA): (1) the effect of the position, the effect of calcium concentration level, as well as the interaction between calcium concentration level and position and (2) the effect of time, the effect of calcium concentration level, as well as the interaction between calcium concentration level and time. Multiple measurements per subject generally result in the correlated errors that are explicitly forbidden by the assumptions of standard (between-subjects) ANOVA. Mixed effects models flexibly give correct estimates of fixed effects in the presence of the correlated errors that arise from a data hierarchy, by controlling for the effects of individual and eventual nested effects. Student T-tests were used for *post hoc* comparisons with Bonferroni correction to account for multiple testing. Diagrams and values presented in the text show mean and standard error with significance levels of p values indicated as follow: *:$p < 0.05$; **:$p < 0.01$; ***:$p < 0.001$. Statistical analyses and figures were performed using R version 2.13.0 (R Core Team (2013). R: a language and environment for statistical computing. R Foundation for Statistical Computing, Vienna, Austria).

Results

Electric current circuit is generated around cell membrane wounds

Xenopus laevis oocyte wounding. First, we established a method to induce reproducible wounds as described in the materials and methods section. After wounding, the area of the wound decreased from 4528.2 ± 310 μm^2 at +1 min to 648.2 ± 115.5 μm^2 at +15 min (ESI,† Fig. S1) illustrating the relatively fast cell membrane wound healing. We next measured the endogenous electric current density at the intact cell membrane and at cell membrane wounds during the healing process under control condition using the vibrating probe.

Wounds generate an electric current circuit. A large inward electric current was detected at the wound center one minute after cell membrane wounding, (−39.4 ± 2.8 μA cm^{-2}). A smaller inward current at the wound edge (−4.8 ± 1.1 μA cm^{-2}) and an outward current at the wound side (100 μm from the edge; 2.7 ± 0.4 μA cm^{-2}; Fig. 1A–C, ESI,† Table S1) were also measured. The ANOVA revealed a significant effect of position on electric current density, and *post hoc* analysis revealed highly significant difference when compared with control values (0.7 ± 0.05 μA cm^{-2}; all $p < 0.001$) illustrating the spatial dynamics of the wound electric current circuit (Fig. 1D).

We made the same measurements at more distant points (starting at mid distance between animal pole and marginal zone) and found the electric current density was not significantly different before and after wounding (at +1 min; ESI,† Fig. S2), suggesting that wounding may not affect electric current density at the cell membrane far from the wound beyond a quarter of the animal–vegetal pole axis (Fig. 1D).

The electric current circuit generated by wounds is maintained before decreasing slowly. We next measured the electric current density at the wound center and wound side during the healing process. Both at wound center and wound side under control condition, we observed a slight increased current and then a gradual decrease until finally returning to close to the intact cell membrane value (Fig. 2A and C, ESI,† Table S1). ANOVA revealed a significant effect of time on electric currents density ($p < 0.001$) illustrating the temporal dynamics of the wound electric current.

Cell membrane is depolarized upon wounding and gradually re-polarizes during healing

The inward electric current observed at the wound center suggests an entry of positive charges into the cell that could depolarize the cell membrane. To test this hypothesis, we used an oocyte patch-clamp system. After wounding under control condition, membrane potential was significantly depolarized from −35.0 ± 0.6 mV in intact membrane to −13.2 ± 0.3 mV

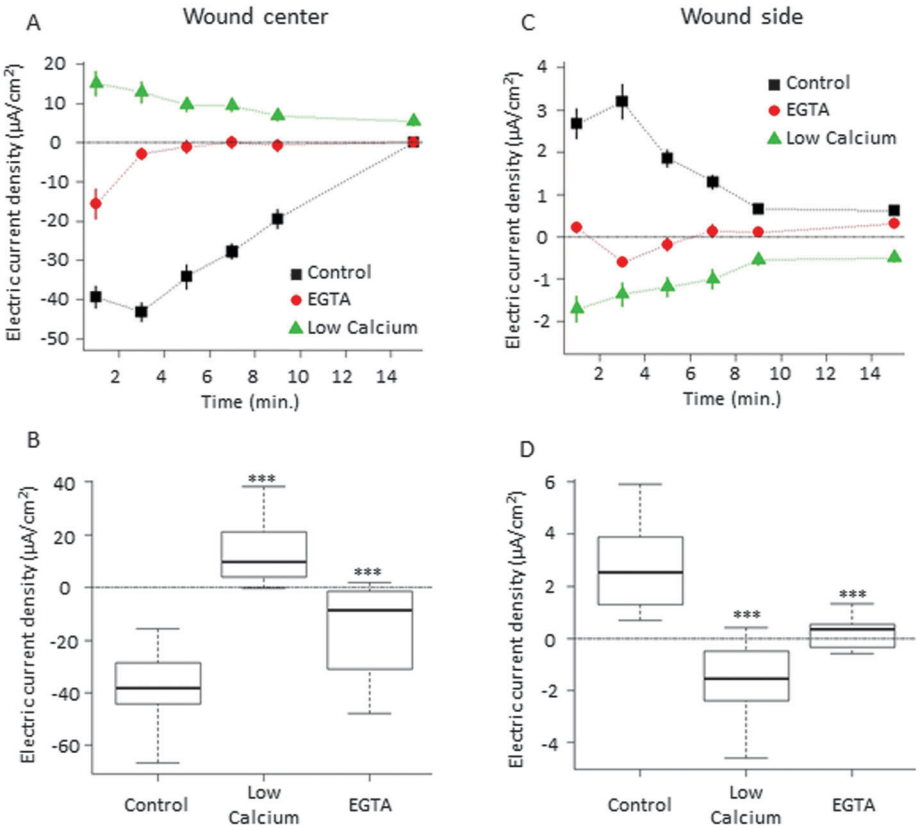

Fig. 2 Extracellular calcium is required for electric current circuit formation and maintenance. (A) Diagram showing means and standard error of wound center electric current density at different times in control condition (black squares, n = 21), in presence of 5 mM EGTA (red dots, n = 20) or in presence of low extracellular calcium concentration (green triangles, n = 20). Again, as in Fig. 1, positive values represent outward current, negative values show inward current. (B) Box plot showing wound center electric current density distributions one minute after wounding in the same conditions as (A). (C) Diagram showing means and standard error of wound side electric current density at wound side at different times in control condition (black squares, n = 18), in presence of 5 mM EGTA (red dots, n = 19) or in presence of low extracellular calcium concentration (green triangles, n = 19). (D) Box plot showing wound side electric current density distributions one minute after wounding in the same conditions as (C).

(+1 min, $p < 0.001$; see Fig. 3A, B, D and E) and gradually repolarized until the cell membrane re-sealed (Fig. 3A, B, D and F; ESI,† Table S2), illustrating the dynamics of cell membrane potential during cell membrane re-sealing.

Calcium flux into the wound decreases as the wound heals

The cell membrane depolarization observed upon wounding could suggests an influx of a positively charged molecules, such as ions. Interestingly, calcium, that bears two positive charges, is the ion that has been identified to play an essential role during cell membrane re-sealing[4a,c,18] and the bathing solution, MMR 1×, has over fifteen times higher calcium concentration (0.6 mM) than that inside the cell (0.04 mM).[15a] We decided to test if an influx of calcium appears after wounding. To test this hypothesis, we used the ion selective electrode to measure calcium flux in control condition.

Calcium flow in the cell through the wounds. One to two minutes after wounding we detected a large influx of calcium (-176.7 ± 24.6 nM cm^{-2} s^{-1}) compared to a small influx of calcium at the intact membrane (-5.2 ± 0.4 nM cm^{-2} s^{-1}; Fig. 4C and D and ESI,† Fig. S3B). Then, during healing, the influx of calcium decreases to finally stabilize (Fig. 4C; ESI,† Table S3). ANOVA revealed a significant effect of time on calcium flux measures ($p < 0.001$).

Calcium flux at the wound sides is not affected by wounding. Influx of calcium measured at the wound side between one and two minutes after wounding did not significantly change during cell membrane re-sealing ($p = 0.31$; ESI,† Fig. S4A and B). In addition, the wound side calcium influx was not significantly different from that measured at the intact membrane ($p = 0.9$; ESI,† Fig. S4C and Table S3). These results suggest that the *Xenopus laevis* oocyte cell membrane wounding does not affect calcium influx at intact membrane outside the wound.

Extracellular calcium is required for cell membrane re-sealing

We then decided to test the requirement of extracellular calcium for wound electric current density, cell membrane potential and wound healing. In order to test this, we incubated the oocytes in solutions that contained lower (low calcium or EGTA) extracellular calcium concentrations compared to control (see Materials and methods for details).

First, we decide to test if modulations of extracellular calcium concentration affect *Xenopus laevis* oocyte cell membrane re-sealing in our wound healing assay. Starting with similar

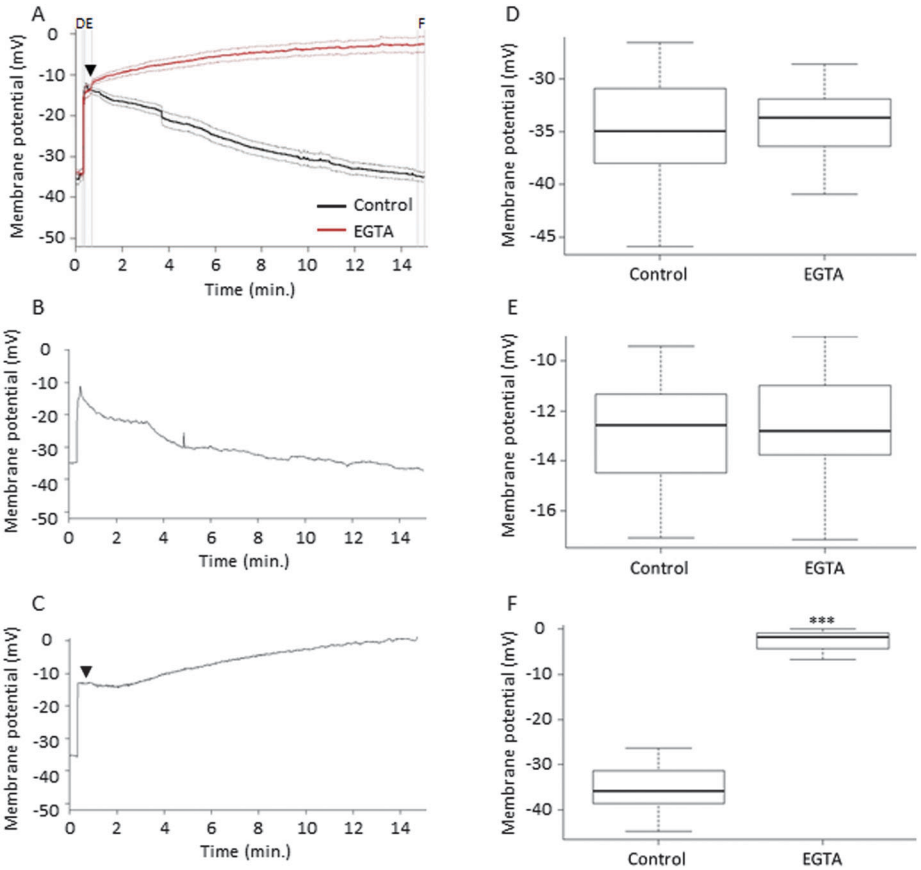

Fig. 3 Extracellular calcium is required for cell membrane re-polarization. (A) Diagram showing means (solid lines) and standard error (dashed lines) of *Xenopus laevis* oocyte cell membrane potential measurements before and after wounding over time in control conditions (black lines, n = 19) or in the presence of 5 mM EGTA (red lines, n = 22). Wound was made thirty seconds after the measurement starts and EGTA added thirty seconds after wounding (arrow head). Letters show positions used to measure data shown in graphs (D–F). (B) and (C) Example of *Xenopus laevis* oocytes cell membrane potential measurements prior and after wounding over the time in control condition (B) or after addition of 5 mM EGTA (C). (D–F) Box plots showing the distribution of *Xenopus laevis* oocytes cell membrane potential measurements over a 20 seconds period prior to wounding (D), ten second after wounding (E) and fifteen minutes after the recording start in the same conditions as in (A).

wound areas (ESI,† Fig. S1A–C), we observed that decreasing extracellular calcium concentration resulted in a strong and significant inhibition of wound healing compared with control calcium concentration ($p < 0.001$; ESI,† Fig. S1A, B and D).

Extracellular calcium is required for calcium influx through the wounds

Second, we tested if reduction of extracellular calcium concentration affects calcium flux at the intact membranes and at the wounds.

ANOVA revealed a significant effect of extracellular calcium concentration ($p < 0.001$) on calcium flux measured at the intact cell membrane and after wounding. *Post hoc* analyses revealed significantly reduced calcium influx for low calcium solutions as compared with control concentration at the intact membrane ($p < 0.001$; ESI,† Fig. S3 and Table S4), at the level of the wound center ($p < 0.001$; Fig. 4 and ESI,† Table S4) and at the level of the wound sides ($p < 0.01$; ESI,† Fig. S4C and Table S4). Surprisingly, compared with control concentration, the presence of EGTA was found to have a less dramatic effect on calcium influx measurements at intact cell membrane ($p = 0.075$; ESI,† Fig. S3 and Table S4) and at the wound center ($p = 0.049$, Fig. 4 and ESI,† Table S4).

Extracellular calcium is required for electric current circuit formation and maintenance

We have confirmed that reduction of extracellular calcium concentration inhibits wound healing and calcium influx. We then tested its effects on the electric current at the intact membrane and on the dynamics of wound electric current circuitry during healing.

Reduction of extracellular calcium concentration does not affect electric current density at the intact membrane. We did not see any significant effects of calcium concentration on electric current density in the intact membrane ($p = 0.17$) but did measure a significant effect of the position ($p < 0.001$), independently of the calcium concentration level ($p = 0.44$, ESI,† Fig. S5).

Extracellular calcium is required for the formation of the electric current circuit. We found a significant effect of both calcium concentration and position on current density, as well as a significant interaction between the two variables (all $p < 0.001$).

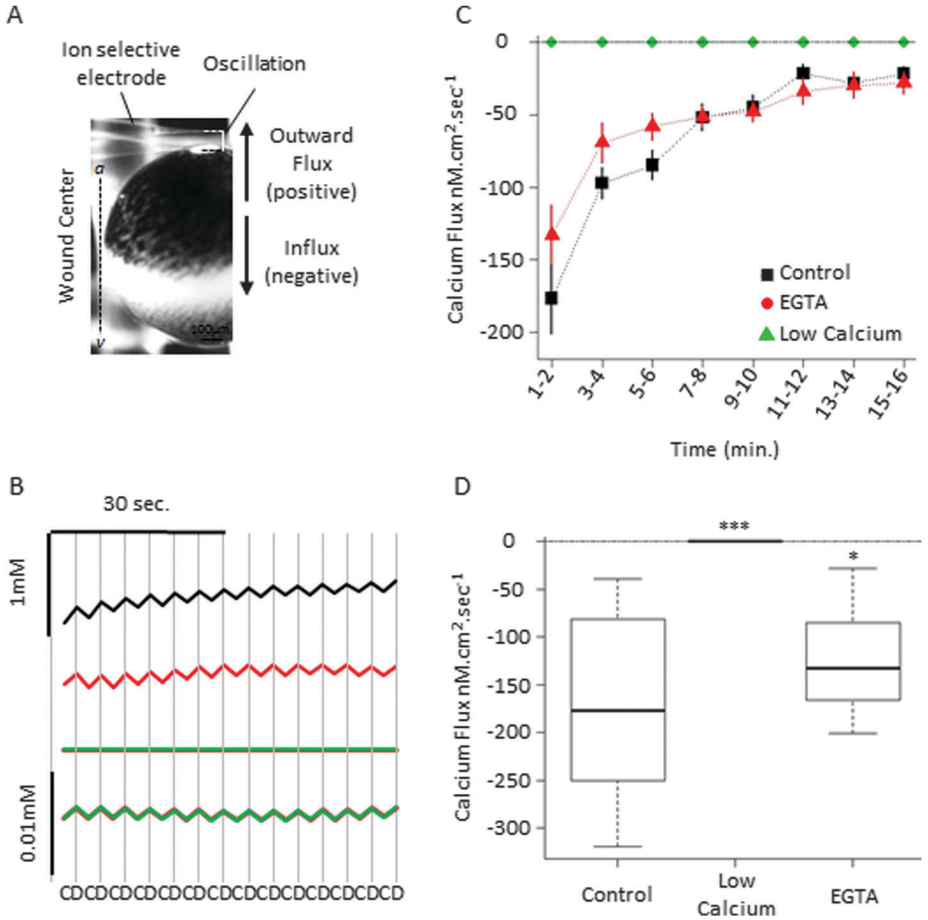

Fig. 4 Extracellular calcium is required for calcium influx through the wounds. (A) Photograph illustrating the calcium flux measurements at cell membrane wound center. Arrows indicates the direction of the calcium flux represented by positive value when outflow and negative value when influx in (C) and (D). (B) Example of calcium selective electrode measurement traces obtained at the wound center one minute after wounding in control condition (black), in presence of 5 mM EGTA (red) or in presence of low extracellular calcium concentration (green). (C) Diagram showing means and standard error of calcium flux at different times in control condition (black squares, n = 15), in presence of 5 mM EGTA (red dots, n = 8) or in presence of low extracellular calcium concentration (green triangles, n = 16). (D) Box plot showing wound center calcium flux distributions one minute after wounding in the same conditions as (C).

Post hoc analyses revealed that one minute after wounding, low extracellular calcium concentrations were found to inhibit or reverse the inward electric current at the wound center (Fig. 2A and B; ESI,† Table S1) and to inhibit or reverse the outward electric current at the wound sides (Fig. 2C and D; ESI,† Table S1).

Extracellular calcium is required for the maintenance of the electric current circuit. Interestingly, the electric current density remained at a high level up to five minutes after wounding in normal calcium concentration, while it remains very small or reversed at the wound center (Fig. 2A; ESI,† Table S1) and at the wound sides (Fig. 2C; ESI,† Table S1) in decreased extracellular calcium concentration. These results suggest that, during re-sealing, extracellular calcium concentration is required for the maintenance of the electric current circuit around cell membrane wounds.

Extracellular calcium is required for cell membrane re-polarization

We then decided to test if the calcium influx observed at the level of the wound could control the cell membrane potential at the intact membrane and its dynamic during healing.

Low extracellular calcium depolarizes the intact cell membrane. Although starting from similar initial cell membrane potential values, reduction of extracellular calcium resulted in a strong depolarization as compared with that observed with the control (ESI,† Fig. S6 and Table S5). Interestingly, while in control, cell membrane potential remains stable; in EGTA conditions, it remains depolarized (ESI,† Fig. S6 and Table S5).

Cell membrane re-polarization during healing requires extracellular calcium. Starting from similar membrane potential values in the different conditions, oocytes were wounded causing cell membranes to depolarize (Fig. 3A–D; ESI,† Table S2). Reduction of extracellular calcium concentration by addition of EGTA resulted in a fast, significant and permanent depolarization compared with the normal calcium concentration where the membrane potential gradually repolarized during cell membrane re-sealing (Fig. 3A–C and F; ESI,† Table S2). These results suggest that extracellular calcium, and calcium flux into the wound, are required for cell membrane re-polarization during *Xenopus laevis* oocyte wound healing.

Discussion

Calcium influx controls wound electric current circuitry and cell membrane potential dynamics

In this article, we identify and describe for the first time the dynamics of electric current circuitry, cell membrane potential and calcium influx during *Xenopus laevis* oocyte wound healing. In addition, we show calcium influx requirements for wound electric current circuitry and cell membrane re-polarization.

We have shown that upon cell membrane wounding, an inward electric current appears at the wound center and an outward electric current appears at its sides, forming a wound electric current circuitry (Fig. 5A). Interestingly, the density of the electric current is maintained during the first minutes of healing, before decreasing slowly (Fig. 5). In addition, we have shown that upon wounding cell membrane is quickly depolarized and then gradually re-polarized during healing (Fig. 5). The observed inward electric current at the level of the wound and the cell membrane depolarization could be due to the entry of positively charged ions such as calcium. We tested this hypothesis and showed that a calcium influx appears at the wound level while no differences in calcium flux were observed at the wound sides compare to control (Fig. 5). These data suggest that the movement of the calcium ion "per-se" at wound center could be responsible for the inward electric current observed at the level of the wound and for cell membrane depolarization while it may not be responsible for the outward electric current observed at wound sides. However, the calcium flux observed at the level of the wound decreases rapidly after wounding, in contrast to the electric current that is maintained for the first minutes of healing (Fig. 5). This suggests that the movement of the calcium ion "per-se" at the wound may not be responsible for the maintenance of the density of the electric current circuitry during the first minutes of healing.

Thus, we tested if extracellular calcium is regulating the dynamic of wound electric current circuitry and membrane potential. First, we measured the calcium flux at the level of the wound when extracellular calcium concentration was decreased. We incubated the oocytes in 2 different solutions that contained (1) about sixteen times less calcium (low calcium) than the control solution and (2) a chelator of calcium ion, EGTA. As expected, a decreased extracellular calcium concentration (low calcium) leads to a decreased influx of calcium. Surprisingly, calcium fluxes were not modified (or only slightly modified) by EGTA, unlike the wound healing, electric current density and cell membrane potential, which were modulated by EGTA (ESI,† Table S6). EGTA and low calcium solutions demonstrated similar effects on wound healing and wound electric current (ESI,† Table S1 and S6). These observations suggest that (i) EGTA did bind calcium, reducing extracellular calcium concentration and resulting in the observed electrophysiological dysregulations, and (ii) the ionophore used in those experiments (see ion selective electrode measurements in materials and methods section) might be detecting calcium that is bound to EGTA, resulting in calcium concentration measurements in EGTA similar to control solution, although these suggestions need to be further tested.

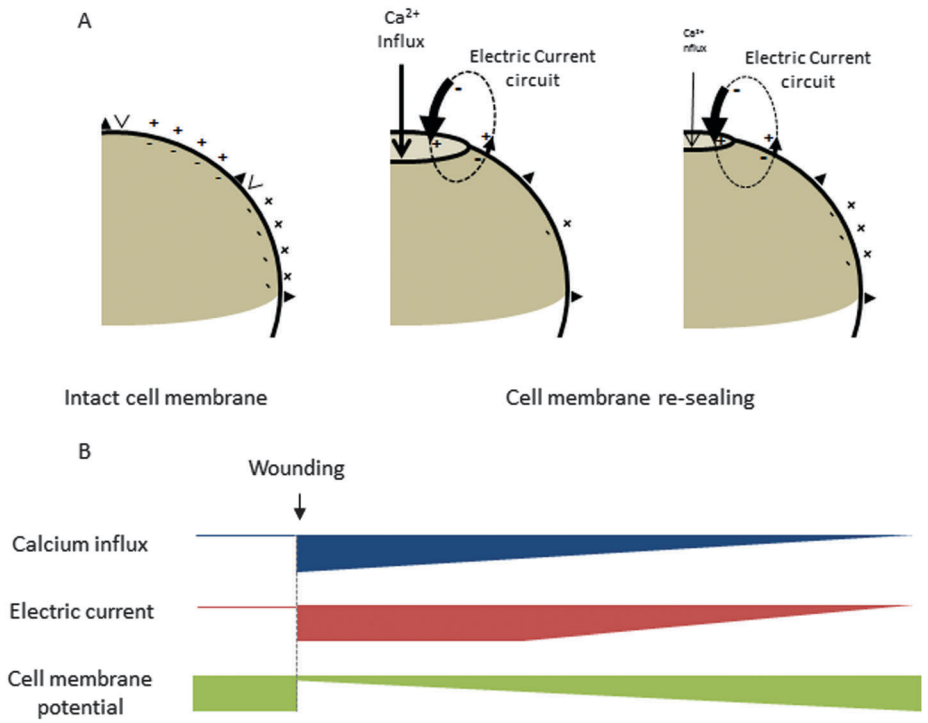

Fig. 5 Dynamics of single cell wound electric current circuitry, cell membrane potential and calcium influx during healing. (A) Schematic illustrating the spatial dynamics of electric current circuitry, cell membrane potential and calcium influx prior to wounding and during healing. (B) Diagram illustrating the temporal dynamics of calcium influx and electric current at the wound center and cell membrane potential during healing.

Second, we measured the electric current density when extracellular calcium concentration was decreased. Reduction of extracellular calcium decreased both the inward electric current at the wound center and reversed the outward current at the wound sides at all times during healing (ESI,† Table S6). Those data show that the calcium influx through the wound is required for the dynamics of electric current circuitry. Interestingly, when extracellular calcium concentration is reduced the electric current density remains small or reversed (ESI,† Table S6). Because the influx of calcium is reduced rapidly, the calcium ion ''per-se'' could not maintain the electric current density. Thus, it is suggested that the calcium that enters through the wounds activates a mechanism in the cell that allows the maintenance of the electric current intensity during the first minutes of healing.

Third, we measured the cell membrane potential when extracellular calcium concentration was reduced. Decreased calcium after wounding leads to cell membrane depolarization (less negative inside; ESI,† Table S6). Decreasing the entry of a positive ion into the cell should lead to a cell membrane becoming more polarized. Surprisingly, we observe the opposite in the case of calcium. These data could suggest that calcium activates a molecular mechanism that compensates for the entry of positively charge ions, allowing repolarization of the membrane (for example, modulation of calcium- or voltage-sensitive ion channels).

The wound electric current circuitry and cell membrane potential variation are likely carried by the passive or active movements of other ions such as sodium or chloride as in the cornea wounds.[19]

Regulation of electric current and membrane polarization by active ion transport

The discrepancy between calcium flux at and around the wound during cell membrane re-sealing and its electrophysiological effects lead us to suggest that it could not only act as a charge molecule that participates in electrophysiological manifestation due to its movement but also participates as a signaling cue, an activator of molecular mechanisms that in turn regulate cell membrane re-sealing and the electrophysiological status of the cell. In addition to the rise in intracellular calcium, the depolarization of the cell membrane could also play this role. Variations of intra- and extra-cellular calcium concentration and cell membrane potential are known to control the activity of specific ion channels expressed at the cell membrane. What are the channels that could control wound electric current and membrane potential dynamics downstream of calcium during single cell wound healing?

Chloride channels outnumber by far all other ion conductances of the oocyte plasma membrane.[20] Four classes of chloride channels have been described so far and one group may be important, the calcium activated chloride channels (CaCCs).

When the membrane wound is made we observed an influx of calcium in addition to cell membrane depolarization. Interestingly, an increased intracellular calcium concentration is known to induce a chloride current that is potentiated by cell membrane depolarization.[15c,d] In addition, wounding plasma membrane in starfish oocytes induced a rapid increase in chloride permeability, which was suggested to be mediated by the fusion of chloride-permeable intracellular membranes with plasma membrane.[6] Our data, in the light of those articles, suggest that the influx of calcium together with cell membrane depolarization could induce a flux of chloride that could participate in regulating wound electric current circuitry and cell membrane potential dynamics. Excitingly, calcium activated chloride channels (CaCCs) are expressed in *Xenopus laevis* oocytes and more concentrated at the animal hemisphere, where the wounds here were made. CaCCs create a functional polarity that plays important roles during further developmental changes following fertilization.[15c,21] In addition, CaCCs have been identified as key regulators of wound electric current and wound healing in rat cornea (Reid and Zhao, unpublished data). CaCCs in the oocytes are modulated by phosphorylation and protein kinase C (PKC)[22] and can be inhibited by several chloride channel blockers such as niflumic acid, flufenamic acid, 9-AC (anthracene-9-carboxylic acid) and NPPB,[15e,23] opening the possibility to study the requirements of CaCCs for *Xenopus laevis* oocyte wound healing and their impact on the dynamics of wound electric current circuitry and cell membrane potential during healing. A CaCC, termed TMEM16A or ANO1, was recently shown to be present in the *Xenopus* oocyte[24] and a specific inhibitor[25] and activator[26] can be used to modulates its activity. In the future, it would be interesting to test if TMEM16A controls downstream calcium influx, cell membrane re-sealing and the dynamics of wound electric current circuitry and cell membrane potential during healing.

Conclusion

To conclude, we have shown that calcium is a key regulator of the wound electric current circuitry and cell membrane potential during healing. Immediately after wounding the calcium influx at the level of the wound controls the electric current intensity, a role that may be supported by its movement as a charge molecule and that could also participate in cell membrane depolarization. In addition, we show that despite a rapid reduction of the calcium influx at the wound center, calcium is required for the maintenance of the wound electric current circuitry and cell membrane re-polarization. Those roles may be supported by calcium as an activator of molecular mechanisms such as ion channel activation that more directly control those processes.

Acknowledgements

This work was supported by National Science Foundation grant MCB-0951199, and in part by the California Institute of Regenerative Medicine grant RB1-01417. We are grateful to Dr Tsung-Yu Chen for help and suggestions on whole cell measurement. The authors declare that they have no competing financial interests.

References

1 (*a*) K. J. Sonnemann and W. M. Bement, Wound repair: toward understanding and integration of single-cell and multicellular wound responses, *Annu. Rev. Cell Dev. Biol.*, 2011, **27**, 237–263, DOI: 10.1146/annurev-cellbio-092910-154251;

(*b*) P. L. McNeil and R. A. Steinhardt, Plasma membrane disruption: repair, prevention, adaptation, *Annu. Rev. Cell Dev. Biol.*, 2003, **19**, 697–731, DOI: 10.1146/annurev.cellbio.19.111301.140101.

2 M. T. Abreu-Blanco, J. M. Verboon and S. M. Parkhurst, Single cell wound repair: Dealing with life's little traumas, *BioArchitecture*, 2011, **1**, 114–121, DOI: 10.4161/bioa.1.3.17091.

3 B. M. Burkel, H. A. Benink, E. M. Vaughan, G. von Dassow and W. M. Bement, A Rho GTPase signal treadmill backs a contractile array, *Dev. Cell*, 2012, **23**, 384–396, DOI: 10.1016/j.devcel.2012.05.025.

4 (*a*) W. M. Bement, C. A. Mandato and M. N. Kirsch, Wound-induced assembly and closure of an actomyosin purse string in Xenopus oocytes, *Curr. Biol.*, 1999, **9**, 579–587; (*b*) C. A. Mandato and W. M. Bement, Contraction and polymerization cooperate to assemble and close actomyosin rings around Xenopus oocyte wounds, *J. Cell Biol.*, 2001, **154**, 785–797, DOI: 10.1083/jcb.200103105; (*c*) H. A. Benink and W. M. Bement, Concentric zones of active RhoA and Cdc42 around single cell wounds, *J. Cell Biol.*, 2005, **168**, 429–439, DOI: 10.1083/jcb.200411109; (*d*) C. M. Simon, E. M. Vaughan, W. M. Bement and L. Edelstein-Keshet, Pattern formation of Rho GTPases in single cell wound healing, *Mol. Biol. Cell*, 2013, **24**, 421–432, DOI: 10.1091/mbc.E12-08-0634.

5 (*a*) R. B. Borgens, Voltage gradients and ionic currents in injured and regenerating axons, *Adv. Neurol.*, 1988, **47**, 51–66; (*b*) T. L. Krause, H. M. Fishman, M. L. Ballinger and G. D. Bittner, Extent and mechanism of sealing in transected giant axons of squid and earthworms, *J. Neurosci.*, 1994, **14**, 6638–6651.

6 A. Fein and M. Terasaki, Rapid increase in plasma membrane chloride permeability during wound resealing in starfish oocytes, *J. Gen. Physiol.*, 2005, **126**, 151–159, DOI: 10.1085/jgp.200509294.

7 (*a*) M. Poo and K. R. Robinson, Electrophoresis of concanavalin A receptors along embryonic muscle cell membrane, *Nature*, 1977, **265**, 602–605; (*b*) L. F. Jaffe, Electrophoresis along cell membranes, *Nature*, 1977, **265**, 600–602.

8 (*a*) J. Stollberg and S. E. Fraser, Acetylcholine receptors and concanavalin A-binding sites on cultured Xenopus muscle cells: electrophoresis, diffusion, and aggregation, *J. Cell Biol.*, 1988, **107**, 1397–1408; (*b*) N. Orida and M. M. Poo, Electrophoretic movement and localisation of acetylcholine receptors in the embryonic muscle cell membrane, *Nature*, 1978, **275**, 31–35.

9 M. S. Cooper, J. P. Miller and S. E. Fraser, Electrophoretic repatterning of charged cytoplasmic molecules within tissues coupled by gap junctions by externally applied electric fields, *Dev. Biol.*, 1989, **132**, 179–188.

10 R. I. Woodruff and W. H. Telfer, Electrophoresis of proteins in intercellular bridges, *Nature*, 1980, **286**, 84–86.

11 T. Fukumoto, I. P. Kema and M. Levin, Serotonin signaling is a very early step in patterning of the left-right axis in chick and frog embryos, *Curr. Biol.*, 2005, **15**, 794–803, DOI: 10.1016/j.cub.2005.03.044.

12 T. Yeung, G. E. Gilbert, J. Shi, J. Silvius, A. Kapus and S. Grinstein, Membrane phosphatidylserine regulates surface charge and protein localization, *Science*, 2008, **319**, 210–213, DOI: 10.1126/science.1152066.

13 M. Zhao, Electrical fields in wound healing-An overriding signal that directs cell migration, *Semin. Cell Dev. Biol.*, 2009, **20**, 674–682, DOI: 10.1016/j.semcdb.2008.12.009.

14 M. T. Abreu-Blanco, J. M. Verboon and S. M. Parkhurst, Cell wound repair in Drosophila occurs through three distinct phases of membrane and cytoskeletal remodeling, *J. Cell Biol.*, 2011, **193**, 455–464, DOI: 10.1083/jcb.201011018.

15 (*a*) C. C. Petersen and G. Dupont, The initiation of a calcium signal in Xenopus oocytes, *Cell Calcium*, 1994, **16**, 391–403; (*b*) J. D. Horisberger, V. Lemas, J. P. Kraehenbuhl and B. C. Rossier, Structure-function relationship of Na,K-ATPase, *Annu. Rev. Physiol.*, 1991, **53**, 565–584, DOI: 10.1146/annurev.ph.53.030191.003025; (*c*) R. Miledi and I. Parker, Chloride current induced by injection of calcium into Xenopus oocytes, *J. Physiol.*, 1984, **357**, 173–183; (*d*) A. Kuruma and H. C. Hartzell, Dynamics of calcium regulation of chloride currents in Xenopus oocytes, *Am. J. Physiol.*, 1999, **276**, C161–C175; (*e*) Z. Qu and H. C. Hartzell, Functional geometry of the permeation pathway of Ca2+-activated Cl-channels inferred from analysis of voltage-dependent block, *J. Biol. Chem.*, 2001, **276**, 18423–18429, DOI: 10.1074/jbc.M101264200; (*f*) I. Parker and R. Miledi, A calcium-independent chloride current activated by hyperpolarization in Xenopus oocytes, *Proc. R. Soc. London, Ser. B*, 1988, **233**, 191–199.

16 B. Reid, R. Nuccitelli and M. Zhao, Non-invasive measurement of bioelectric currents with a vibrating probe, *Nat. Protoc.*, 2007, **2**, 661–669, DOI: 10.1038/nprot.2007.91.

17 B. Reid and M. Zhao, Ion-selective self-referencing probes for measuring specific ion flux, *Commun. Integr. Biol.*, 2011, **4**, 524–527, DOI: 10.4161/cib.4.5.16182.

18 R. A. Steinhardt, G. Bi and J. M. Alderton, Cell membrane resealing by a vesicular mechanism similar to neurotransmitter release, *Science*, 1994, **263**, 390–393.

19 (*a*) B. Reid, A. C. Vieira, L. Cao, M. J. Mannis, I. R. Schwab and M. Zhao, Specific ion fluxes generate cornea wound electric currents, *Commun. Integr. Biol.*, 2011, **4**, 462–465, DOI: 10.4161/cib.4.4.15545; (*b*) A. C. Vieira, B. Reid, L. Cao, M. J. Mannis, I. R. Schwab and M. Zhao, Ionic components of electric current at rat corneal wounds, *PLoS One*, 2011, **6**, e17411, DOI: 10.1371/journal.pone.0017411.

20 K. Sobczak, N. Bangel-Ruland, G. Leier and W. M. Weber, Endogenous transport systems in the Xenopus laevis oocyte plasma membrane, *Methods*, 2010, **51**, 183–189, DOI: 10.1016/j.ymeth.2009.12.001.

21 (*a*) R. Miledi, A calcium-dependent transient outward current in Xenopus laevis oocytes, *Proc. R. Soc. London, Ser. B*, 1982, **215**, 491–497; (*b*) M. Lupu-Meiri, H. Shapira and Y. Oron, Hemispheric asymmetry of rapid chloride responses to inositol trisphosphate and calcium in Xenopus oocytes, *FEBS Lett.*, 1988, **240**, 83–87; (*c*) J. M. Gomez-Hernandez, W. Stuhmer and A. B. Parekh, Calcium dependence and distribution of calcium-activated chloride

channels in Xenopus oocytes, *J. Physiol.*, 1997, **502**(Pt 3), 569–574.

22 (*a*) K. Hahnenkamp, M. E. Durieux, H. van Aken, S. Berning, T. J. Heyse, C. W. Honemann and B. Linck, Modulation of Xenopus laevis Ca-activated Cl currents by protein kinase C and protein phosphatases: implications for studies of anesthetic mechanisms, *Anesth. Analg.*, 2004, **99**, 416–422, DOI: 10.1213/01.ANE.0000121351.38401.AB; (*b*) R. Boton, D. Singer and N. Dascal, Inactivation of calcium-activated chloride conductance in Xenopus oocytes: roles of calcium and protein kinase C, *Pfluegers Arch.*, 1990, **416**, 1–6; (*c*) M. J. Kim, Y. S. Lee and J. K. Han, Modulation of lysophosphatidic acid-induced Cl- currents by protein kinases A and C in the Xenopus oocyte, *Biochem. Pharmacol.*, 2000, **59**, 241–247.

23 (*a*) G. Wu and O. P. Hamill, NPPB block of Ca(++)-activated Cl- currents in Xenopus oocytes, *Pfluegers Arch.*, 1992, **420**, 227–229; (*b*) M. M. White and M. Aylwin, Niflumic and flufenamic acids are potent reversible blockers of Ca2(+)-activated Cl- channels in Xenopus oocytes, *Mol. Pharmacol.*, 1990, **37**, 720–724.

24 B. C. Schroeder, T. Cheng, Y. N. Jan and L. Y. Jan, Expression cloning of TMEM16A as a calcium-activated chloride channel subunit, *Cell*, 2008, **134**, 1019–1029, DOI: 10.1016/j.cell.2008.09.003.

25 W. Namkung, P. W. Phuan and A. S. Verkman, TMEM16A inhibitors reveal TMEM16A as a minor component of calcium-activated chloride channel conductance in airway and intestinal epithelial cells, *J. Biol. Chem.*, 2011, **286**, 2365–2374, DOI: 10.1074/jbc.M110.175109.

26 W. Namkung, Z. Yao, W. E. Finkbeiner and A. S. Verkman, Small-molecule activators of TMEM16A, a calcium-activated chloride channel, stimulate epithelial chloride secretion and intestinal contraction, *FASEB J.*, 2011, **25**, 4048–4062, DOI: 10.1096/fj.11-191627.

